Monthly Notices of the ROYAL ASTRONOMICAL SOCIETY

MNRAS **444,** 558–565 (2014) doi:10.1093/mnras/stu1463

H I in the Arp 202 system and its tidal dwarf candidate

Chandreyee Sengupta,[1⋆] T. C. Scott,[2] K. S. Dwarakanath,[3] D. J. Saikia[4,5] and B. W. Sohn[1,6]

[1]*Korea Astronomy and Space Science Institute, 776 Daedeokdae ro, Yuseong gu, Daejeon 305-348, Republic of Korea*
[2]*Centre for Astrophysics Research, University of Hertfordshire, College Lane, Hatfield AL10 9AB, UK*
[3]*Raman Research Institute, Bangalore 560 080, India*
[4]*National Centre for Radio Astrophysics, Tata Institute of Fundamental Research, Pune 411 007, India*
[5]*Cotton College State University, Panbazar, Guwahati 781 001, India*
[6]*Department of Astronomy and Space Science, University of Science and Technology, 217 Gajeong ro, Daejeon 305-350, Republic of Korea*

Accepted 2014 July 21. Received 2014 July 21; in original form 2014 April 21

ABSTRACT

We present results from our Giant Metrewave Radio Telescope (GMRT) H I observations of the interacting pair Arp 202 (NGC 2719 and NGC 2719A). Earlier deep ultraviolet (*Galaxy Evolution Explorer*) observations of this system revealed a tidal-tail-like extension with a diffuse object towards its end, proposed as a tidal dwarf galaxy (TDG) candidate. We detect H I emission from the Arp 202 system, including H I counterparts for the tidal tail and the TDG candidate. Our GMRT H I morphological and kinematic results clearly link the H I tidal tail and the H I TDG counterparts to the interaction between NGC 2719 and NGC 2719A, thus strengthening the case for the TDG. The Arp 202 TDG candidate belongs to a small group of TDG candidates with extremely blue colours. In order to gain a better understanding of this group we carried out a comparative study of their properties from the available data. We find that H I (and probably stellar) masses of this extremely blue group are similar to the lowest H I mass TDGs in the literature. However the number of such blue TDG candidates examined so far is too small to conclude whether or not their properties justify them to be considered as a subgroup of TDGs.

Key words: galaxies: dwarf – galaxies: individual: Arp 202 – galaxies: interactions – galaxies: kinematics and dynamics – galaxies: spiral – radio lines: galaxies.

1 INTRODUCTION

Tidal interactions between galaxies, where at least one of them is gas rich, can result in tidal stripping of large amounts of H I from the potential of the parent galaxy(s). Most of this stripped H I will eventually fall back into the potential of one or other of the interacting galaxies or be incorporated into the intragroup medium (IGM). However, if the H I densities are sufficient and environmental conditions are favourable, self-gravitating bodies with masses typical of dwarf galaxies, called tidal dwarf galaxies (TDG), may form within the tidally stripped gas (Duc & Mirabel 1999; Duc et al. 2000). Apart from establishing that these are indeed self-gravitating objects, a key observational problem is to distinguish TDGs from older standard dwarfs because some TDGs contain old stars stripped from their parent galaxies. Other TDGs consist almost entirely of young stars formed in situ from H I stripped from the parents during the interaction (Duc & Mirabel 1999; Duc et al. 2000; Braine et al. 2001). A combination of evidence linking the TDG candidate to interacting parents and stellar population studies is normally used to identify TDG candidates, although indisputable criteria remain to be accepted.

TDGs are usually observed during an active star-forming stage thus allowing tests of star formation criteria and stellar to gas relationships in low gas density environments. As TDGs form from stripped gas they are expected to contain little or no dark matter (Elmegreen, Kaufman & Thomasson 1993). This makes them valuable in studying the role and importance of dark matter in galaxy formation. TDGs are also expected to be metal rich in comparison to normal dwarfs, because the gas from which TDGs form originates from more evolved, usually large, late-type galaxies. The lack of dark matter in TDG's implies they are more vulnerable to disruption by further tidal interactions than normal dwarfs. Thus TDGs provide a unique environment to investigate the processes governing formation and evolution of galaxies.

To address the issue of in situ star and TDG formation in tidal gas debris, a multiwavelength study of a sample of Arp interacting galaxies [the 'Spirals, Bridges and Tails' (SB&T) sample] is being carried out (Smith et al. 2007, 2010a). *Galaxy Evolution Explorer* (*GALEX*), *Spitzer* and Hα observations of these systems

⋆E-mail: sengupta.chandreyee@gmail.com

have revealed evidence of in situ star formation and TDG candidates. One such system is the Arp 202 close pair of galaxies, NGC 2719 and NGC 2719A, which have radial velocities 3077 and 3117 km s^{-1}, respectively, and signs of a tidal interaction at optical and ultraviolet (UV) wavelengths (Figs 1 and 2). Deep UV *(GALEX)* observations of this system revealed a tidal-tail-like extension which appears to originate from NGC 2719A with a diffuse object towards its end, proposed as a TDG by Smith et al. (2010a).

In this paper, we present results from our Giant Metrewave Radio Telescope (GMRT) H I observations of the Arp 202 system including at the position of the proposed TDG. The paper also utilizes publicly available Sloan Digital Sky Survey (SDSS), *Spitzer* and *GALEX* data and images. Section 2 sets out details of our observations, and the results are given in Section 3. We discuss the results in Section 4. A summary and concluding remarks are set out in Section 5. The average of the radial velocities of NGC 2719 and NGC 2719A is 3097 km s^{-1}. Using this average velocity and assuming H_0 to be 75 km s^{-1} Mpc^{-1}, we adopt a distance of 41.3 Mpc for NGC 2719, NGC 2719A and the TDG. At this distance the spatial scale is 12 kpc arcmin^{-1}. J2000 coordinates are used throughout the paper, including in the figures.

2 OBSERVATIONS

H I observations of Arp 202 were carried out with the GMRT on 2008 April 30. Further details of the observations are given in Table 1. The baseband bandwidth used was 8 MHz for the H I 21-cm line observations giving a velocity resolution of ∼13 km s^{-1}.

The Astronomical Image Processing System (AIPS) software package was used for data reduction. Bad data from malfunctioning antennas, antennas with low gain and/or radio frequency interference (RFI) were flagged. The flux densities are on the scale of Baars et al. (1977), with flux density uncertainties of ∼5 per cent. Following calibration, continuum subtraction was carried out in the *uv* domain using the AIPS tasks UVSUB and UVLIN. To analyse the H I structures, image cubes of different resolutions were produced by applying different 'tapers' to the data with varied *uv* limits. The task IMAGR was then used to obtain the final cleaned H I image cubes. The integrated H I and H I velocity field maps were extracted from the cubes using the AIPS task MOMNT. Details for the final high- and low-resolution cubes are given in Table 1.

3 OBSERVATIONAL RESULTS

The contours in Fig. 1 are from the low-resolution (47.5 × 37.4 arcsec^2) integrated H I GMRT map for the Arp 202 field overlaid on a SDSS *g-*, *r-*, *i*-band false colour image. H I properties of the objects for the Arp 202 field are set out in Table 2. The two principal H I detections are, the large SABc spiral, NGC 2724, in the north-east and the Arp 202 system in the west detected in the velocity range 2942–3238 km s^{-1}. Within the Arp 202 system the main features are the H I counterparts of the near-UV (NUV;*GALEX*)

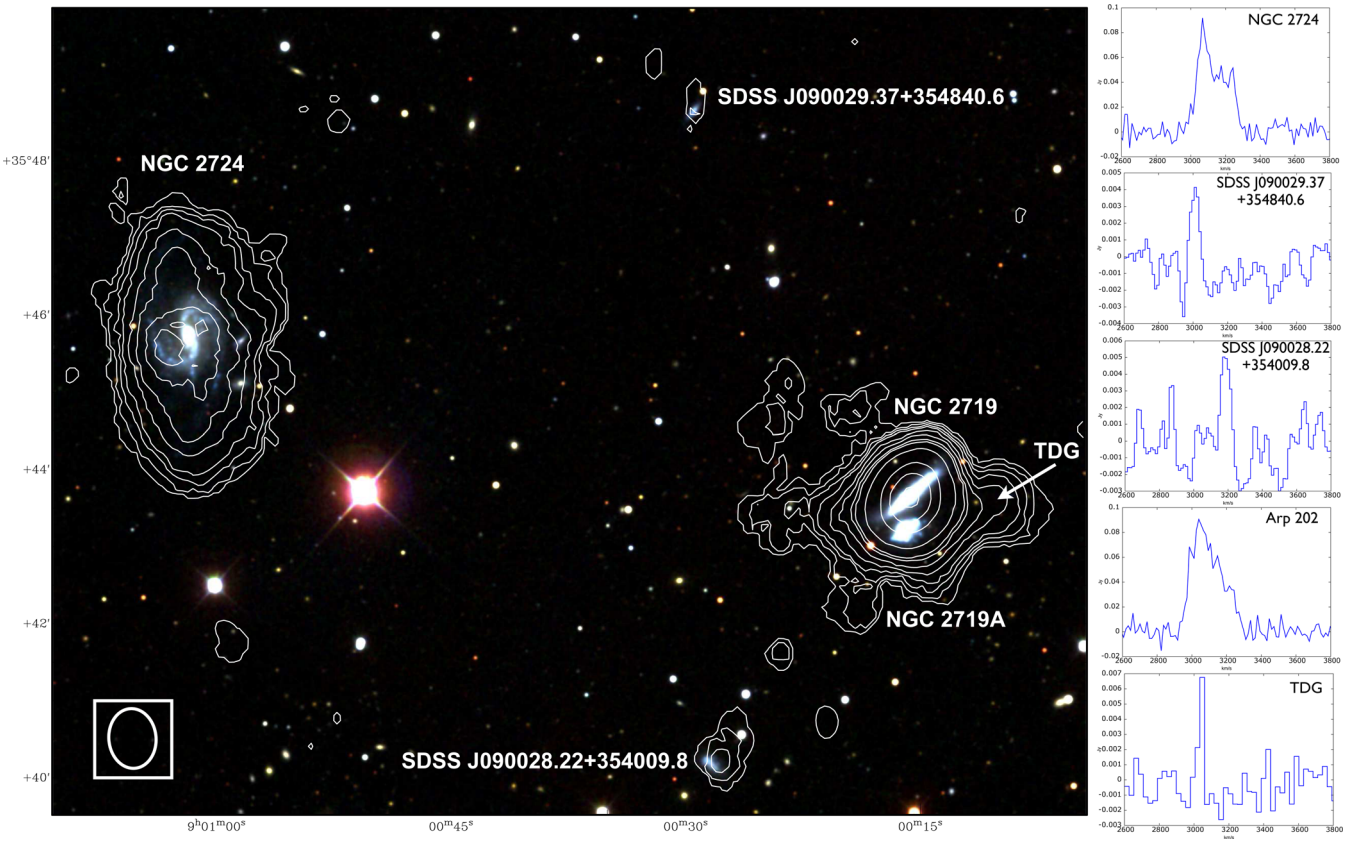

Figure 1. Arp 202 field: left: low-resolution integrated H I emission contours overplotted on a SDSS *g-*, *r-*, *i*-band false colour image. The contours are H I column density levels of 10^{19} atoms cm^{-2} × (4.4, 9.3, 15.5, 21.7, 34.1, 46.5, 61.9, 71.2, 105.3, 185.8, 247.7, 309.7). The first contour is at 3σ. The beam size (47.5 × 37.4 arcsec^2) is indicated by the ellipse at the bottom left of the image. Names of galaxies detected in H I are shown adjacent to their optical positions. Right: GMRT H I spectra, with a velocity resolution of 27 km s^{-1}, for each of the detections. The Arp 202 spectrum is from the integrated emission from NGC 2719, NGC 2719A, the tidal tail and the TDG candidate.

Table 1. GMRT observation details.

Frequency	1420.4057 MHz
Observation date	2008 April 30
Primary calibrator	3C 147
Phase calibrator (flux density)	0741+312 (2.00 Jy)
Integration time	8.0 hours
Primary beam	24 arcmin at 20 cm
Low-resolution beam	47.5×37.4 arcsec^2 (PA $= 5\overset{\circ}{.}9$)
High-resolution beam	23.4×16.3 arcsec^2 (PA $= 17\overset{\circ}{.}8$)
rms for low-resolution map	1.24 mJy beam^{-1}
rms for high-resolution map	0.81 mJy beam^{-1}
RA (pointing centre)	$09^{\rm h}00^{\rm m}17\overset{\rm s}{.}17$
Dec. (pointing centre)	$35^\circ43'33\overset{''}{.}12$

tidal tail and TDG candidate. Fig. 2 shows the high-resolution (23.5×16.3 arcsec^2) H I integrated map contours overlaid on a NUV (*GALEX*) image of the two principal galaxies in Arp 202 system and the TDG candidate. Fig. 2 which shows the tidal tail–TDG connection at H I column densities $\gtrsim 4.3\times10^{20}$ cm^{-2}. The peak H I column density found at the position of the TDG candidate is $\sim 7.5\times10^{20}$ cm^{-2}. In the channel images (Fig. 3) the H I tail is visible from velocities 2995 to 3076 km s^{-1} and the H I peak emission in the tail coincides with the TDG in the velocity range of 3022–3049 km s^{-1}. The projected length of the H I tidal tail which appears to originate from NGC 2719A is $\sim$1.5 arcmin (20 kpc).

Apart from the galaxies referred to in the previous paragraph, two further galaxies were detected in H I within the full width at half-maximum (FWHM) of the GMRT primary beam: SDSS J090028.22+354009.8 projected $\sim$4.1 arcmin to the south-east of the Arp 202 and SDSS J090029.37+354840.6 projected $\sim$5.9 arcmin to the north-east of Arp 202. SDSS J090029.37+354840.6 was marginally detected (Fig. 1), however, the spectrum and channel maps show the H I signal to be correlated in consecutive channels at the optical position of the galaxy. We therefore conclude the H I is associated with optical galaxy.

The GMRT spectrum for each of the galaxies detected in H I and the Arp 202 system is plotted on the right-hand side of Fig. 1. The GMRT integrated flux density from the Arp 202 system is 17.55 Jy km s^{-1}, which compares well with the uncorrected single-dish flux density of 16.70 Jy km s^{-1} for NGC 2719

Table 2. GMRT H I detections.

Object	RA ($^{\rm h}:^{\rm m}:^{\rm s}$)	Dec. ($^\circ:'':''$)	Velocity H I (km s^{-1})	M(H I) $\times 10^9$ ($M_\odot$)
Arp 202 pair				7.1 ± 0.3
NGC 2719	09:00:15.4	+35:43:40		
NGC 2719A	09:00:15.9	+35:43:12		
TDG candidate	09:00:09.3	+35:43:38	3047 ± 13.6	0.1 ± 0.05
NGC 2724	09:01:01.8	+35:45:43	3220 ± 13.6	5.6 ± 0.4
SDSS J090029.37+354840.6	09:00:29.4	+35:48:41	3081 ± 13.6	$\leq$0.1
SDSS J090028.22+354009.8	09:00:28.2	+35:40:10	3301 ± 13.6	$\leq$0.1

Note: Uncertainties on H I masses quoted here are for an adopted distance and inclination angle, estimated using uncertainty on the line flux. Actual uncertainties on the masses can be higher.

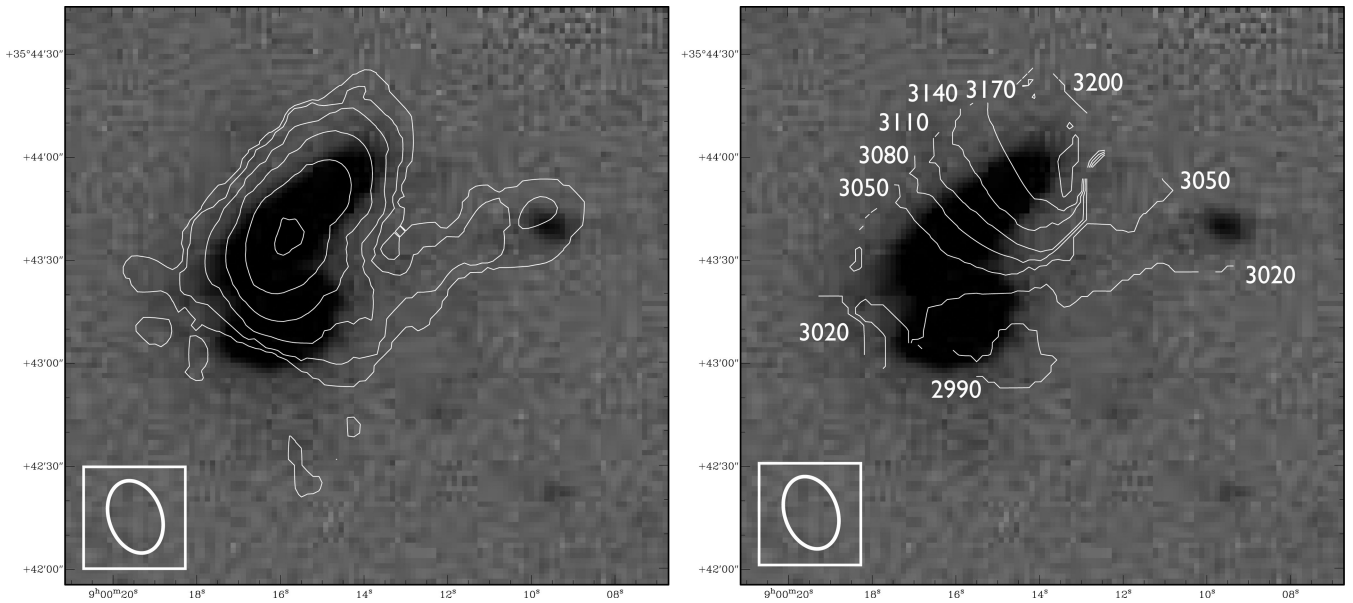

Figure 2. Arp 202: left-hand panel: high-resolution H I integrated map contours (white) overlaid on a NUV *(GALEX)* image. The H I column density contour levels are 10^{20} atoms cm^{-2} $\times$ (4.4, 7.5, 14.5, 26.0, 43.4, 66.6). Right-hand panel: H I velocity with contours at velocity separation of 30 km s^{-1}. The H I beam (23.4×16.3 arcsec^2) is shown as white ellipse at the bottom left of each panel.

(Huchtmeier & Richter 1989). The H I mass derived from the GMRT for the Arp 202 pair, tidal tail and the candidate TDG is $7.1 \pm 0.3 \times 10^9$ M$_\odot$. We extracted an H I spectrum from within approximately a 23×16 arcsec^2 region (similar to the beam) centred on the TDG (Fig. 2) and derived an H I mass for the TDG of $\sim 1 \pm 0.5 \times 10^8$ M$_\odot$. The integrated flux density from the GMRT spectrum of NGC 2724 is 13.9 Jy km s^{-1} which compares well with the single-dish value of 13.8 Jy km s^{-1} (Springob et al. 2005). SDSS J090028.22+354009.8, which is ∼49 kpc to the south-east of the Arp pair, shows signatures of interaction in H I maps and is connected to the pair by a very faint and fragmented H I bridge. The bridge can be traced in the channel images (Fig. 3), although the signal-to-noise ratio is poor.

Fig. 2, right-hand panel, shows the velocity field of the Arp 202 system from the high-resolution cube. The contours between 3050 and 3200 km s^{-1} indicate the H I in the central and north-west parts of the NGC 2719 discis in a regularly rotating edge on disc, although with indications of a warp. This rotation pattern is broken at south-eastern end of the NGC 2719 H I disc at velocities below 3050 km s^{-1}. The abrupt change of rotation pattern in the contours together with the tidal-tail morphology at velocities below 3050 km s^{-1} indicates the H I there has been strongly perturbed by the interaction between NGC 2719 and NGC 2719A. The narrow range of H I velocities, ∼60 km s^{-1}, in the tidal tail running westward from NGC 2719A to and including the TDG candidate provide clear evidence linking the both the tidal tail and TDG candidate to the interaction between NGC 2719 and NGC 2719A.

4 DISCUSSION

4.1 Arp 202 – major interactions

The pre-merger interacting pair, NGC 2719 and NGC 2719A, have an optical radial velocity separation of 40 km s^{-1} and D_{25} of 1.3 arcsec (17.5 kpc) and 0.9 arcsec (12 kpc), respectively. We estimate the stellar mass for NGC 2719 at $\sim 3.4 \times 10^9$ M$_\odot$ and NGC 2719A at 5.0×10^9 M$_\odot$ (a stellar mass ratio of ∼1:1.4), based on the parameters from Bell et al. (2003) and Blanton et al. (2003) for SDSS g-band magnitudes and $g - r$ colours. The sizes, SDSS colours and stellar masses indicate these are relatively small late-type galaxies [Im pec per NASA/IPAC Extragalactic Database (NED)]. In optical images NGC 2719 presents as an essentially intact high-inclination disc. While both galaxies are designated as late types, the high-resolution H I channel maps in Fig. 3 show that almost all of the H I emission is projected against the NGC 2719 disc. Despite NGC 2719 having the optical appearance of an edge-on spiral, the GMRT H I spectrum lacks double horned structure expected from a rotating H I disc. This and the tidal perturbation parameter,[1] $p_{gg} = 0.6$, suggest the NGC 2719 H I disc may have been severely perturbed by the interaction between the pair. NGC 2719A has a more irregular optical morphology, and the UV tail (Fig. 2) appears to originate from this galaxy. It seems likely the H I and stellar material in the tidal tail has its origin in a close interaction between NGC 2719 and NGC 2719A, where NGC 2719A has lost most of its H I to NGC 2719 and the IGM.

The Arp 202 pair are H I rich, with a combined H I mass of 7.1×10^9 M$_\odot$. Galaxies of same size and morphological type as NGC 2719 and 2719A are expected to have H I masses of $\sim 2.8 \times 10^9$ and $\sim 1.7 \times 10^9$ M$_\odot$, respectively (Haynes & Giovanelli 1984), making a total of 4.5×10^9 M$_\odot$ for the pair.. The presence of excess H I mass may be due to the system acquiring H I though interactions and/or accretion of small neighbours. A 60-arcmin radius (720 kpc at that distance) search around the Arp 202 system, within a velocity range of 2000–4000 km s^{-1}, yields only one similar-sized neighbour (NGC 2724) and two small dwarfs (SDSS J090028.22+354009.8 and SDSS J090029.37+354840.6). The projected distance between Arp 202 and NGC 2724 is 9.6 arcmin (115 kpc). Assuming galaxies are moving at ∼150 km s^{-1}, a typical number for velocity dispersion in loose groups, we estimate that if they have crossed paths, then the last interaction could have occurred about 3.6×10^8 yr ago, less than the dynamical time-scales of NGC 2719 and NGC 2724, which are estimated to be 4.2×10^8 and 5.2×10^8 yr, respectively. Had there been an interaction involving a massive transfer of H I between these two galaxies, extended tidal features would have remained in the H I discs for at least one dynamical time-scale. While the H I in Arp 202 is heavily perturbed, the NGC 2724 H I disc is relatively undisturbed and shows no significant H I deficiency. The expected H I mass of NGC 2724 is 2.9×10^9 M$_\odot$ (Haynes & Giovanelli 1984) compared to the observed mass of $5.6 \pm 0.4 \times 10^9$ M$_\odot$, making it an H I-rich spiral. Thus even if it has interacted with the Arp 202 system, it seems unlikely that any massive gas exchange has taken place between them. We conclude that the perturbation signatures in the Arp 202 are primarily the result of the interaction between NGC 2719 and NGC 2719A.

4.2 SDSS J090028.22+354009.8 and SDSS J090029.37+354840.6 – minor interactions

Apart from NGC 2724, there are two dwarfs close to the Arp 202 system. SDSS J090028.22+354009.8, to the south-east is ∼4.1 arcmin (49 kpc) away and SDSS J090029.37+354840.6 to the north-east is ∼5.8 arcmin (69 kpc) away. Their stellar masses were estimated from the SDSS photometric measurements quoted in NED and using the mass to light ratio to colour relation prescribed in Bell et al. (2003). The value for solar absolute magnitude in g band was taken from Blanton et al. (2003). The stellar masses for SDSS J090028.22+354009.8 and SDSS J090029.37+354840.6 are estimated as 3.9×10^9 and 1.1×10^8 M$_\odot$, respectively. Their H I masses from the GMRT data are estimated to be $\leq 1 \times 10^8$ M$_\odot$. The upper limit was applied as they both are not unambiguously 3σ detections. Both the galaxies are beyond the fields imaged by *Spitzer* and only SDSS J090028.22+354009.8 is within the *GALEX* Medium Imaging Survey (MIS) field. The galaxy is bright in the *GALEX* map indicating star formation activity within the last 10^8 yr. This is not unexpected as SDSS J090028.22+354009.8 shows signs of recent interaction with the Arp 202 system. We have detected fragments of an H I bridge connecting Arp 202 and SDSS J090028.22+354009.8. We see no similar H I connection between Arp 202 and SDSS J090029.37+354840.6. But we notice an offset between the optical and the H I radial velocities for both these galaxies. While SDSS J090028.22+354009.8 and SDSS J090029.37+354840.6 have optical velocities of 3301 and 3081 km s^{-1} in NED, the H I is detected at velocities ∼3181 and 3011 km s^{-1}, respectively. The H I velocities quoted here correspond to the peak intensities. The H I line widths at 20 per cent

[1] $p_{gg} = \frac{(M_{comp}/M_{gal})}{(d/r_{gal})^3}$ (Byrd & Valtonen 1990), where M_{gal} (5×10^9 M$_\odot$) and M_{comp} (3.4×10^9 M$_\odot$) are the masses of the galaxy and companion, respectively, d is the separation (0.461 arcmin) and r is the galaxy disc optical radius (0.45 arcmin). Values of $p_{gg} > 0.1$ are likely to lead to tidally induced star formation.

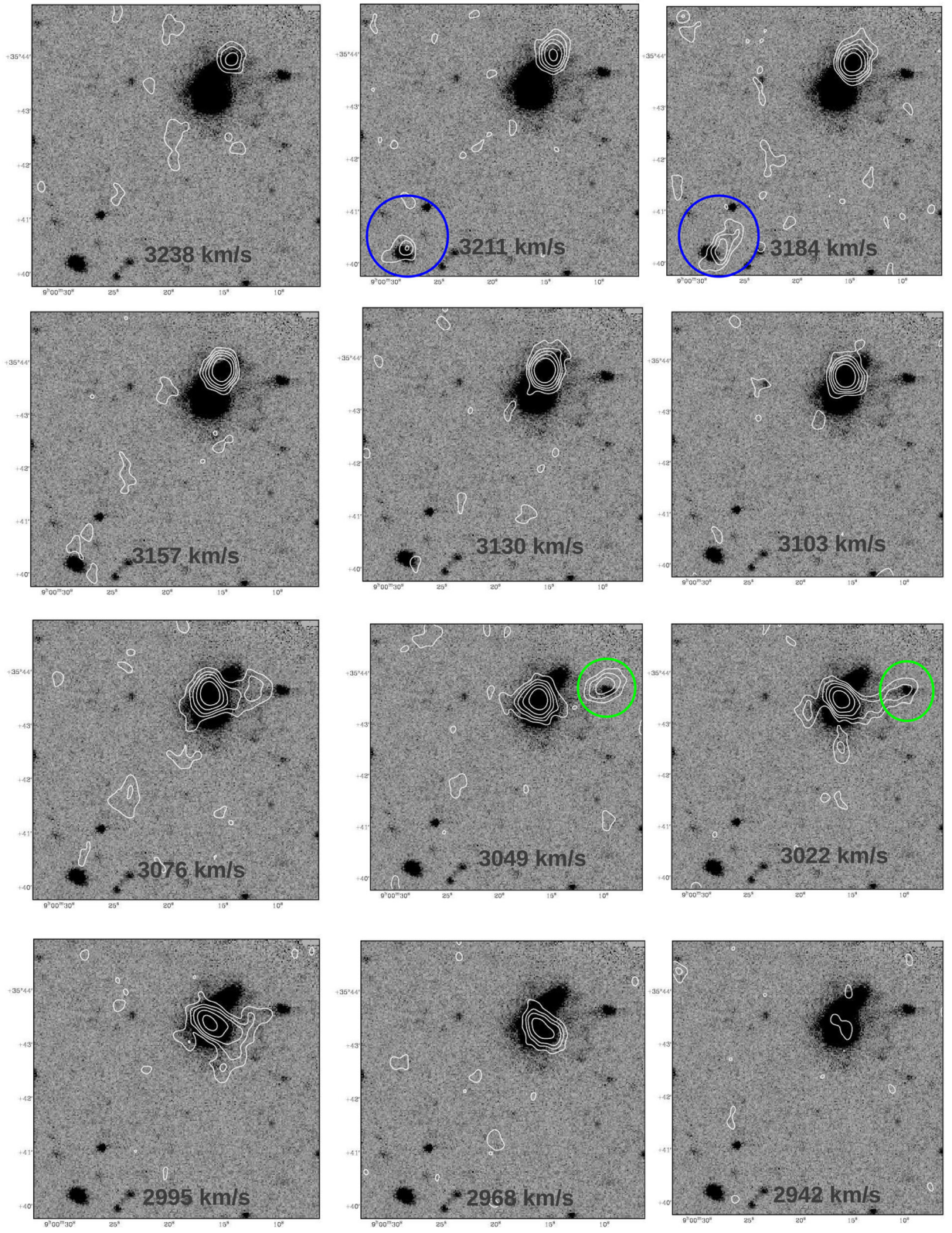

Figure 3. Channel images from the high-resolution cube (beam is 23.4 × 16.3 arcsec^2) showing the Arp 202 pair, the candidate TDG (indicated by green circle) and the fragmented H I bridge between Arp 202 and SDSS J090028.22+354009.8 (indicated by blue circle). The contour levels are 0.7 mJy × (3, 5, 7, 10, 15). The H I contours are overlayed on the SDSS *r*-band image.

of the peak flux value of SDSS J090028.22+354009.8 and SDSS J090029.37+354840.6 are 109 and 82 km s^{-1}, respectively. This shift of the H I velocity could be due to interactions with the Arp 202 system, during which the gas discs of the smaller galaxies have been disturbed. Also H I loss from these galaxies to the Arp 202 system cannot be ruled out.

Since it is difficult to establish if such nearby dwarfs are indeed TDGs, we compared the available information on these galaxies to those of TDGs and probed the chances of them being Arp 202 system detached TDGs. Judging by the optical and H I masses and the SDSS $g - r$ colours, SDSS J090028.22+354009.8 seems to be an old dwarf galaxy associated with the Arp 202 system. Its $g - r$ colour is an extreme 1.65, much higher than usual early-type dwarfs making it an unreliable number to derive concrete conclusions. SDSS J090029.37+354840.6 on the other hand is a bluer dwarf, with $g - r$ value as 0.19, which is considered low in dwarf galaxy samples (Barazza et al. 2006) and similar to blue compact dwarf galaxies (BCDG; Zitrin, Brosch & Bilenko 2009). In terms of stellar populations, tidal dwarf galaxies are known to be of two types, one with extremely new stars, with optical colours similar to BCDGs and the other dominated by an older population, mostly derived from the fragments of the parent galaxies (Duc & Mirabel 1999). However, the dynamical mass to gas mass ratio of SDSS J090029.37+354840.6 is ∼8. Because of the predicted absence of dark matter, this ratio is expected to be closer to 1 in TDGs. Additionally, the galaxy is about 70 kpc away from the main system and previous studies about TDG detachment show that 95 per cent of TDGs are found within 20 kpc of their parent system (Kaviraj et al. 2012). Thus from the information available we conclude these dwarfs are not detached TDGs, but rather old satellites of the system. Metallicity and CO data for these dwarfs could further constrain the origin of these dwarfs.

4.3 The candidate TDG of the Arp 202 system

Smith et al. (2010b) first reported the presence of a clumpy star-forming tidal tail terminating in the TDG candidate from NUV (*GALEX*) observations and confirmed the candidate was part of the Arp 202 system with optical spectroscopy. Our GMRT H I morphology and kinematic results, set out in Section 3, clearly show that the H I tidal tail/bridge links the H I TDG counterpart to the interacting Arp 202 pair.

The tail and TDG candidate are faintly visible in individual SDSS images but are much more apparent in the UV *(GALEX)* images. Neither were detected in either the *Spitzer* 8 μm or Southeastern Association for Research in Astronomy (SARA) Hα images. This lead Smith et al. (2010b) to suggest that the TDG may be in a post-starburst stage, i.e. dominated by a stellar population with age between 10^7 and 10^8 yr. Schechtman-Rook & Hess (2012) presented a FUV $- g$ versus $g - r$ plot (their fig. 11) for the UV-detected TDG candidates from the Smith et al. (2010b) and two other candidates, Holmberg IX and NGC 4656UV. The Arp 202 TDG candidate appears in their plot as one of the candidates with extreme blue colour, together with NGC 4656UV, Arp 305 and Holmberg IX, one of the strongest TDG candidates (Sabbi et al. 2008). The mean FUV $- g$ colour of these four TDG candidates (blue candidates) is close to 0, ∼1 mag lower than the rest of the Smith et al. (2010b) sample. But as Schechtman-Rook & Hess (2012) point out a larger sample is needed to determine whether the blue candidates are part of a separate category of TDGs. While acknowledging this limitation, in Table 3, we compare selected properties of the Arp 202 TDG candidate with those of the other three blue candidates and statistics from larger samples of TDG candidates (Duc & Mirabel 1999; Kaviraj et al. 2012). The aim of compiling the data in the table was to determine if the blue candidates share any additional distinguishing features. In the following paragraphs we briefly comment sequentially on each row in Table 3.

In Table 3 the mass and size estimates, in particular, are highly uncertain, so we are only able to draw order of magnitude conclusions from their comparative data. The uncertainties are particularly acute for the estimates of stellar mass (M*). M* in units of 10^8 M$_\odot$ for Arp 202 (0.2) and NGC 4656UV (0.4) were estimated using g- and r-band colours following the method described in footnote '*a*' to Table 3. M* for Holmberg XI (0.02) and Arp 305 (0.04) are taken from the literature (see Table 3 for references) and they were determined from spectral energy distribution (SED) fitting in the respective papers. For Arp 305 M* determined with the g- and r-band colour method is 1.1×10^8 M$_\odot$ suggesting this method may overestimate M* by at least an order of magnitude. The g and r colour M* method assumes the galaxy has a standard mix old and young stellar populations but we have evidence from the non-detections of the Arp 202 TDG candidate in *Spitzer* 3.6, 4.5 and 8 μm images (and only marginal equivalent detections for Arp 305) that these two candidates are relatively deficient in old stellar populations compared to standard galaxies.

From the GMRT spectrum for the Arp 202 TDG candidate (Fig. 1, bottom right-hand panel) we estimate its H I mass to be $\sim 1.0 \times 10^8$ M$_\odot$. The mean $M_{\rm H\,I}$ of the blue candidates is $2.2 \pm 1.6 \times 10^8$ M$_\odot$ which is an order of magnitude lower than the mean value from [$n = 20$] Duc & Mirabel (1999) sample (16×10^8 M$_\odot$). $M_{\rm H\,I}$ for all the blue candidates is close to the minimum $M_{\rm H\,I}$ of 2.0×10^8 M$_\odot$ in Duc & Mirabel (1999) sample. So even allowing for the uncertainties in the estimates of $M_{\rm H\,I}$, the blue candidates have a significantly lower $M_{\rm H\,I}$ than a typical TDG candidate. Moreover, if our interpretation of stellar mass in the previous paragraph is correct, then Arp 202 probably shares a $M_{\rm H\,I}/M$* ratio, of several tens to a hundred or so, with the other blue candidates.

For the Arp 202 TDG candidate, $M_{\rm dyn}$ is estimated at 3.9×10^8 M$_\odot$ using the method described in Table 3. This is ∼4 times the $M_{\rm H\,I} + M$* with a ratio of the same order as in NGC 4656UV. We have no $M_{\rm dyn}$ for Holmberg IX or Arp 305. As for the Arp 202 TDG candidate, we see no clear indication of the presence of significant amounts of dark matter.

Table 3 shows the estimated extent of each of the blue candidates, which range from 2.2 to 11 kpc. Because of the wide range in angular scales and distances to the blue candidates it is difficult to properly compare the extent of these candidates. Moreover, there is also a problem of separating the TDG and tail. We have estimated the extent of the blue candidates from inspection of UV (*GALEX*) images, except for the nearest candidate, Holmberg IX, where we use the value from NED. We concluded that the extent of the blue candidates is typically a few kpc.

From the FUV (*GALEX*) magnitudes (Smith et al. 2010a) and using the star formation rate (SFR) versus far-UV (FUV) luminosity relation in Salim et al. (2007), the estimated SFR of the Arp 202 TDG is 0.039 M$_\odot$ yr^{-1}. This is lower than the mean value of SFRs found in TDGs (Duc & Mirabel 1999). With its gas reserve, at this SFR, the Arp 202 TDG can form stars for more than 2 Gyr. Using the Hα luminosity quoted in Hancock et al. (2009) and the SFR recipe in Kennicutt (1998), we also estimated the SFR for Arp 305 TDG as 0.025 M$_\odot$ yr^{-1}. The SFR values of other blue TDG candidates were taken from the literature (Sabbi et al. 2008; Schechtman-Rook & Hess 2012). The mean SFR for the blue

Table 3. Properties of extremely blue TDGs compared to average properties from literature.

Property	Statistic from TDG candidate samples	Arp 202	NGC 4656UV	Holmberg IX	Arp 305
TDG M^* (10^8 $M_\odot$)[a]		0.2	0.4	0.02	0.04
TDG $M_{H\,I}$ (10^8 $M_\odot$)[b]	16.0[c]	1.0	3.8	3.3	0.6
TDG Mdyn (10^8 $M_\odot$)[d]		3.9	19	–	–
TDG extent (kpc)[e]		4.0	6.3	2.25	11.0
TDG SFR (10^{-3} $M_\odot$ yr^{-1})[f]	79[g]	39	27	8	25
TDG metallicity[h]	8.5[i]	8.9	−1.7	8.5	–
	(12 + log(O/H))	(12 + log(O/H))	[Fe/H]	(12 + log(O/H))	
TDG colour[j]	0.30[k]	0.21	−0.02	−0.07	0.13
colour system	$(B-V)$	$(g-r)$	$(g-r)$	$(g-r)$	$(g-r)$
TDG FUV − g[l]	–	−0.47	0.64	−0.3	0.24
Parent pair mass ratio	>1:7, median = 2.5[m]	1:1.4	1:2.6	1:1.5	1:2.9
TDG projected distance from parent (kpc)[n]	<20[o]	18	11	13	36
TDG estimated age (Myr)[p]	–	–	292	200	–

Note: [a] M^* for Arp 202 and NGC 4656UV are estimated from SDSS g- and r-band colours following $\log(M^*/L_g) = a_g + b_g \times (g-r)$ (Bell et al. 2003) and g-band solar luminosity from parameter from Blanton et al. (2003), using colours from Smith et al. (2010a) and Schechtman-Rook & Hess (2012), respectively. For Holmberg IX M^* is from Sabbi et al. (2008) and M^* for Arp 305 is from Hancock et al. (2009).
[b] $M_{H\,I}$ for Arp 202 from Table 2, NGC 4656UV from Schechtman-Rook & Hess (2012), Holmberg IX from Swaters & Balcells (2002) and Arp 305 from van Moorsel (1983).
[c] Duc & Mirabel (1999).
[d] M_{dyn} for Arp 202 = 3.39×10^4 $a_{H\,I}$ d $(W_{20}/2)$, where $a_{H\,I}$ = diameter in arcmin, d = the distance to the object and W_{20} = the line width at 20 per cent of the peak (Giovanelli & Haynes 1988). The H I beam major axis of the high-resolution map was used as $a_{H\,I}$ and since the signal is present in only two channels in our high-resolution cube, the net width of the two channels was used as W_{20}. NGC 4656UV from Schechtman-Rook & Hess (2012).
[e] Extents were measured from UV (*GALEX*) images except for and Holmberg IX which is from NED.
[f] SFR for the Arp 202 TDG candidate is estimated using the FUV luminosity quoted in Smith et al. (2010a) and the SFR recipe in Salim et al. (2007), NGC 4656UV is from Schechtman-Rook & Hess (2012), Holmberg IX from Sabbi et al. (2008) and SFR for Arp 305 is estimated using the Hα luminosity quoted in Hancock et al. (2009) and the SFR recipe in Kennicutt (1998).
[g] Duc & Mirabel (1999).
[h] Metallicity for: Arp 202 is from Smith et al. (2010a), NGC 4656UV is from Schechtman-Rook & Hess (2012) and Holmberg IX is from Makarova et al. (2002).
[i] Duc & Mirabel (1999).
[j] $g-r$ colour from Smith et al. (2010a), except NGC 4656UV which is converted from table 2 of Schechtman-Rook & Hess (2012).
[k] Duc & Mirabel (1999).
[l] $FUV-g$ colour from Smith et al. (2010a), except NGC 4657UV which is converted from table 2 of Schechtman-Rook & Hess (2012).
[m] Kaviraj et al. (2012).
[n] The projected distances are: for Arp 202 from NGC 2719A, for NGC 4656UV from Schechtman-Rook & Hess (2012), for Holmberg IX from M81 from NED and for Arp 305 from the position of NGC 4017 as per Hancock et al. (2009).
[o] Kaviraj et al. (2012).
[p] The age estimates are: NGC 4656UV from Schechtman-Rook & Hess (2012) and Holmberg XI from Sabbi et al. (2008).

candidates is ∼0.025 $M_\odot$ yr^{-1}, lower than the mean of the Duc & Mirabel (1999) sample. However, we note here that the SFR estimates can significantly change depending on the wavebands. This prevents us from suggesting that the SFRs of the blue candidates are actually lower than the TDG average.

The metallicity for the Arp 202 TDG candidate from Smith et al. (2010a) is log(O/H) + 12 = 8.9, approximately solar metallicity and above the log(O/H) + 12 mean value of the Duc & Mirabel (1999) sample (8.5). We note here that the Arp 202 TDG candidate's spectrum from which the metallicity is quoted is as yet unpublished. Holmberg IX has a similar metallicity to Arp 202 and the Duc & Mirabel (1999) sample but NGC 4656UV is significantly subsolar. Metallicity is one of the strongest tests to distinguish TDGs from standard dwarfs. Higher metallicities are expected if a dwarf formed from metal-rich disc material from a parent galaxy as opposed to the poor metallicities for standard dwarfs formed from pristine gas. Thus the Arp 202 candidate's metallicity provides strong support for it being a TDG, while the NGC 4656UV metallicity value raises a question.

The SDSS $g-r$ colour was calculated using the data from the sources referred to in footnote '*j*' to Table 3. The $g-r$ colour for the Arp 202 candidate is 0.21. As expected from Schechtman-Rook & Hess (2012) results, the mean $g-r$ colour of the blue candidates (0.06 ± 0.13) is bluer than the mean of the six TDG candidates in the Smith et al. (2010a) sample (0.41 ± 0.20). Unfortunately this is not directly comparable to $B-V$ of 0.3 for the 20 TDG candidates in the Duc & Mirabel (1999) sample. The FUV − g colour of the Arp 202 TDG is −0.47, the bluest FUV − g colour amongst the blue candidates.

From a study of TDGs, Kaviraj et al. (2012) concluded that 95 per cent of TDG progenitors are spirals involved in binary mergers where the parent galaxies' mass ratio is less than 1:7 (median 1:2.5). They also concluded TDGs are not produced in interactions where the parent mass ratios exceed 1:11 and for 95 per cent of the time the physical separation between the parent galaxies and the TDG is <20 kpc. These values are consistent with simulations by Bournaud & Duc (2006). For all of the blue candidates including the Arp 202 the progenitor pair mass ratios are within the ratio observed

by Kaviraj et al. (2012). Table 3 shows the protected distance to the nearest gas-rich parent galaxy for three of the blue candidates is within 20 kpc, but the Arp 305 TDG candidate is projected 36 kpc from NGC 4017.

Allowing for the small sample size and measurement uncertainties we see indications that, in addition to the extreme blue colour reported by Schechtman-Rook & Hess (2012), the blue candidates have significant smaller H I masses ($2.2 \pm 1.6 \times 10^8$ $M_\odot$) than the Duc & Mirabel (1999) sample. It seems likely that the stellar masses (M^*) of the blue candidates are commensurately smaller as well. If this is correct, then these candidates would have exceptionally large $M_{H\,I}/M^*$ ratios. The lower mean SFR for the blue candidates compared with the Duc & Mirabel (1999) sample appears, at least in part, to be due to the smaller H I and stellar masses.

5 SUMMARY AND CONCLUDING REMARKS

Our GMRT H I morphology and kinematic results clearly link the H I tidal tail and the H I TDG counterpart to the interaction between NGC 2719 and NGC 2719A. This and the similarity of the Arp 202 candidate's properties to other TDG candidates with extreme blue colours (Table 3), and in particular Holmberg IX, strengthen the case for the Arp 202 candidate being a TDG formed under the standard TDG formation scenario. Observations to estimate molecular gas content and kinematics as well as detailed stellar population analysis could further improve the understanding of the origin of this TDG candidate.

We compared properties of the Arp 202 candidate and three other extremely blue TDG candidates identified by Schechtman-Rook & Hess (2012) to larger samples of TDG candidates. All four of these extremely blue candidates have H I (and probably M^*) masses comparable to the smallest TDGs found in the literature. These lower masses are probably at least partially responsible for the low SFR compared to the Duc & Mirabel (1999) TDG sample. All of the extremely blue candidates are H I rich, with the $M_{H\,I}/M^*$ ratios ranging approximately between 5 and 150. The number of extremely blue TDG candidates examined is too small to conclude whether or not they are a distinct subgroup with TDGs.

ACKNOWLEDGEMENTS

We thank the staff of the GMRT who have made these observations possible. The GMRT is operated by the National Centre for Radio Astrophysics of the Tata Institute of Fundamental Research. This research has made use of the NASA/IPAC Extragalactic Database (NED) which is operated by the Jet Propulsion Laboratory, California Institute of Technology, under contract with the National Aeronautics and Space Administration. CS thanks Dr Yongbeom Kang from KASI for useful discussions.

REFERENCES

Baars J. W. M., Genzel R., Pauliny-Toth I. I. K., Witzel A., 1977, A&A, 61, 99
Barazza F. D. et al., 2006, ApJ, 643, 162
Bell E. F., McIntosh D. H., Katz N., Weinberg M. D., 2003, ApJS, 149, 289
Blanton M. R. et al., 2003, ApJ, 592, 819
Bournaud F., Duc P.-A., 2006, A&A, 456, 481
Braine J., Duc P.-A., Lisenfeld U., Charmandaris V., Vallejo O., Leon S., Brinks E., 2001, A&A, 378, 51
Byrd G., Valtonen M., 1990, ApJ, 350, 89
Duc P.-A., Mirabel I. F., 1999, in Barnes J. E., Sanders D. B., eds, Proc. IAU Symp. 186, Galaxy Interactions at Low and High Redshift. Kluwer, Dordrecht, p. 61
Duc P.-A., Brinks E., Springel V., Pichardo B., Weilbacher P., Mirabel I. F., 2000, AJ, 120, 1238
Elmegreen B. G., Kaufman M., Thomasson M., 1993, ApJ, 412, 90
Giovanelli R., Haynes M. P., 1988, Extragalactic Neutral Hydrogen. Springer-Verlag, Berlin
Hancock M., Smith B. J., Struck C., Giroux M. L., Hurlock S., 2009, AJ, 137, 4643
Haynes M. P., Giovanelli R., 1984, AJ, 89, 758
Huchtmeier W. K., Richter O.-G., 1989, A General Catalog of HI Observations of Galaxies. Springer-Verlag, New York
Kaviraj S., Darg D., Lintott C., Schawinski K., Silk J., 2012, MNRAS, 419, 70
Kennicutt R. C., Jr, 1998, ARA&A, 36, 189
Makarova L. N. et al., 2002, A&A, 396, 473
Sabbi E., Gallagher J. S., Smith L. J., de Mello D. F., Mountain M., 2008, ApJ, 676, 113
Salim S. et al., 2007, ApJS, 173, 267
Schechtman-Rook A., Hess K. M., 2012, ApJ, 750, 171
Smith B. J., Struck C., Hancock M., Appleton P. N., Charmandaris V., Reach W. T., 2007, AJ, 133, 791
Smith B. J., Giroux M. L., Struck C., Hancock M., Hurlock S., 2010a, AJ, 139, 2719
Smith B. J., Giroux M. L., Struck C., Hancock M., Hurlock S., 2010b, in Smith B., Bastian N., Higdon S. J. U., Higdon J. L., eds, ASP Conf. Ser. Vol. 423, Galaxy Wars: Stellar Populations and Star Formation in Interacting Galaxies. Astron. Soc. Pac., San Francisco, p. 257
Springob C. M., Haynes M. P., Giovanelli R., Kent B. R., 2005, ApJS, 160, 149
Swaters R. A., Balcells M., 2002, A&A, 390, 863
van Moorsel G. A., 1983, A&AS, 54, 19
Zitrin A., Brosch N., Bilenko B., 2009, MNRAS, 399, 924

This paper has been typeset from a TEX/LATEX file prepared by the author.